OXFORD

ORIGINAL ARTICLE

Task-Modulated Corticocortical Synchrony in the Cognitive-Motor Network Supporting Handwriting

Timo Saarinen[1,2], Jan Kujala[1,3], Hannu Laaksonen[1,2], Antti Jalava[1] and Riitta Salmelin[1,2]

[1]Department of Neuroscience and Biomedical Engineering, Aalto University, FI-00076 AALTO, Espoo, Finland
[2]Aalto NeuroImaging, Aalto University, FI-00076 AALTO, Espoo, Finland, and [3]Department of Psychology, University of Jyväskylä, FI-40014, Jyväskylä, Finland

Address correspondence to Timo Saarinen, Department of Neuroscience and Biomedical Engineering, Aalto University, P.O. Box 12200, FI-00076 AALTO, Espoo, Finland. Email: timo.p.saarinen@aalto.fi

Abstract

Both motor and cognitive aspects of behavior depend on dynamic, accurately timed neural processes in large-scale brain networks. Here, we studied synchronous interplay between cortical regions during production of cognitive-motor sequences in humans. Specifically, variants of handwriting that differed in motor variability, linguistic content, and memorization of movement cues were contrasted to unveil functional sensitivity of corticocortical connections. Data-driven magnetoencephalography mapping ($n = 10$) uncovered modulation of mostly left-hemispheric corticocortical interactions, as quantified by relative changes in phase synchronization. At low frequencies ($\sim$2–13 Hz), enhanced frontoparietal synchrony was related to regular handwriting, whereas premotor cortical regions synchronized for simple loop production and temporo-occipital areas for a writing task substituting normal script with loop patterns. At the beta-to-gamma band ($\sim$13–45 Hz), enhanced synchrony was observed for regular handwriting in the central and frontoparietal regions, including connections between the sensorimotor and supplementary motor cortices and between the parietal and dorsal premotor/precentral cortices. Interpreted within a modular framework, these modulations of synchrony mainly highlighted interactions of the putative pericentral subsystem of hand coordination and the frontoparietal subsystem mediating working memory operations. As part of cortical dynamics, interregional phase synchrony varies depending on task demands in production of cognitive-motor sequences.

Key words: DICS, functional connectivity, language production, MEG, movement sequence

Introduction

Movement sequences form an essential part of behavior (Lashley 1951; Rhodes et al. 2004; Hogan and Sternad 2007). They prototypically manifest as quasirhythmic, consecutive patterns of either monotonous (e.g., finger tapping and walking) or more varied movement elements (e.g., speaking and handwriting). The cognitive-conceptual frame is thought to support goal-directed movement patterning, realized through higher-order representations of sequences and processes related to internal meaning of the movements (Wolpert and Ghahramani 2000; Hommel et al. 2001; Fuster 2004; Pacherie 2008; Desmurget and Sirigu 2009). Together with subcortical neural elements, such as the basal ganglia and cerebellum, the cerebral cortex contributes significantly to production of organized, meaningful movement sequences (Haaland et al. 2000; Harrington et al. 2000; Tanji 2001). Both motor and cognitive aspects of these sequences are

presumably implemented as dynamic interactions in multifocal, modularly organized networks of cortical regions (e.g., Meunier et al. 2009; Bertolero et al. 2015; Petersen and Sporns 2015).

The present study examined how manipulation of motor and cognitive aspects of a movement sequence task manifests in long-range electrophysiological interactions of the human cortex, as measured with magnetoencephalography (MEG). Here, functional sensitivity of corticocortical connections during sequence production was examined by contrasting variants of a shared root task. We used handwriting as a naturalistic, yet experimentally controllable root task where a cognitive frame guides hand movements. In handwriting, the cognitive frame relates to a verbally coded sequence that is maintained in working memory (see Chenoweth and Hayes 2003; Hayes and Chenoweth 2006). The guidance of movement is presumably mediated through interaction between higher-order representations of the to-be-written sequence and concrete motor patterning, while the motor patterning as such proceeds relatively independently with its own memory buffering (see Ellis 1988; Chenoweth and Hayes 2003; Purcell et al. 2011). A distinction between motor (also referred to as "peripheral") and cognitive ("central") levels of processing has been made for both written and spoken language production (e.g., Purcell et al. 2011; Hickok 2012; Scaltritti et al. 2017). More generally, the cognitive architecture supporting sequential motor performance has been segregated into motor, cognitive, and sensory components (Verwey et al. 2015). In the context of handwriting, this type of division suggests distinct processes for hand coordination, maintenance of the cognitive frame in working memory, and representation of the phonological and visual aspects of written patterns.

We postulated here that these different processing levels broadly align with functio-anatomical subdivisions of the predominantly left-hemispheric representation of handwriting, as estimated on the basis of earlier neuroimaging research (Fig. 1A). This notion is in accordance with general concepts of cortical modularity (Colombo 2013; Crossley et al. 2013; Bertolero et al. 2015). The pericentral subsystem (green; Fig. 1A) associates tightly with hand coordination where the primary hand sensorimotor cortex (SMC) and the supplementary motor area (SMA) form a key substrate for producing movement sequences (Tanji 2001; Haggard 2008; Planton et al. 2013). The dorsal premotor (dPM; so-called Exner's area) and anterior parietal cortices have been associated with spatiomotor specification of writing patterns (Rijntjes et al. 1999; Katanoda et al. 2001; Sugihara et al. 2006; Roux et al. 2009; Kadmon Harpaz et al. 2014), whereas the ventral premotor (vPM) and inferior parietal cortices may contribute to phoneme-to-grapheme conversion (Alexander et al. 1992; Omura et al. 2004; Sugihara et al. 2006) and to tool-use in handwriting (cf. Ramayya et al. 2010; Ishibashi et al. 2016). The frontoparietal subsystem (blue; Fig. 1A) that includes the associative inferior frontal and intraparietal cortices links with domain-general, cognitive-executive processing (Duncan 2010; Barbey et al. 2012; Crossley et al. 2013). This subsystem supports core operations of working memory (Rottschy et al. 2012), including short-term verbal maintenance (Bonhage et al. 2014) and is well suited for representing the cognitive frame of movement sequences (cf. Hommel et al. 2001; Fuster 2004; Shima et al. 2007). The perisylvian-occipital subsystem (red; Fig. 1A) is critically involved in the linguistic and sensory aspects of written language (Purcell et al. 2011; Dehaene et al. 2015; see also Turken and Dronkers 2011; Fedorenko and Thompson-Schill 2014): the posterior temporal cortex has been identified as a key site for

phonological and semantic processes as well as audiovisual letter-sound integration (Raij et al. 2000; van Atteveldt et al. 2004; Roux et al. 2014), while the inferior occipitotemporal cortex crucially represents visual language forms (Tarkiainen et al. 1999; Dehaene et al. 2015; Hannagan et al. 2015).

These functionally specialized clusters of regions (Fig. 1A) were further hypothesized to form a large-scale network system where handwriting is accomplished through interactions between the nodal regions (Fig. 1B). Interactions within and between the subsystems (Fig. 1B; arrows) were further posited to utilize coupled oscillatory signaling as a dynamic mechanism for facilitating distributed, interregional processes (e.g., Bressler et al. 1993; Varela et al. 2001; Fries 2005; Siegel et al. 2012). Functional networks operating at the low end of electrophysiological frequencies (∼1–15 Hz) have been found to support simple hand motor tasks (Gross et al. 2002; Pollok et al. 2005) as well as handwriting (Butz et al. 2006); sensorimotor cortical signaling also coheres with muscle rhythmicity at these frequencies (Gross et al. 2002; Butz et al. 2006; Ruspantini et al. 2012). In separate studies, corticocortical interactions at these low frequencies have further been associated with cognitive tasks, including working memory performance (Sarnthein et al. 1998; Liebe et al. 2012; Watrous et al. 2013) and processing of written language (Kujala et al. 2007). Moreover, the beta (∼13–30 Hz) and gamma bands (>30 Hz) have been both linked with local motor-related cortical activity (e.g., Salmelin et al. 1995; Miller et al. 2012; Cheyne and Ferrari 2013), and they may also convey corticocortical interactions in motor as well as cognitive processes (e.g., Brovelli et al. 2004; Gross et al. 2005; Pesaran et al. 2008; Salazar et al. 2012; Liljeström et al. 2015; Liljeström et al. 2018; Rohenkohl et al. 2018).

The key functional question is how the existing interactions at different neural frequencies manifest sensitivity for each specific task. Phase synchrony of coherently oscillating signals is thought to provide temporal coordination and accuracy to interregional processing in order to facilitate binding and selective linkage of distant processes and to promote efficient mutual communication between regions (Roelfsema et al. 1997; Varela et al. 2001; Siegel et al. 2012; Maris et al. 2016). Behavioral relevance of corticocortical phase synchrony has been demonstrated, for example, in recording of neural activity during memory paradigms in primates (Liebe et al. 2012) and humans (Palva et al. 2010; Watrous et al. 2013), as well as in interventional studies using transcranial stimulation (Polania et al. 2012). The studies registering cortical activity have shown that increasing task-load is reflected as increased phase coupling. Taken this operational principle, we hypothesize that for a complex cognitive-motor task such as handwriting, the multiple interactions in the large-scale cortical network (Fig. 1B) will each have their own sensitivities of phase synchrony related to the different processing levels of the task.

In the present experiment, variants of a handwriting task were contrasted to probe functional sensitivity of corticocortical interactions. These variants (Fig. 1C) included real handwriting of auditorily presented sentences (RW), a sentence writing task where loop patterns substituted the regular script (LW), a sequential drawing task of patterns according to auditory cues (PD), and a simple task of repetitive loop production (LD). All these variants comprised rhythmic hand movements but differed in motor selection (handwriting or varied pattern series versus monotonous loops), linguistic processing (writing vs. drawing tasks), and memory-related task demands (readout
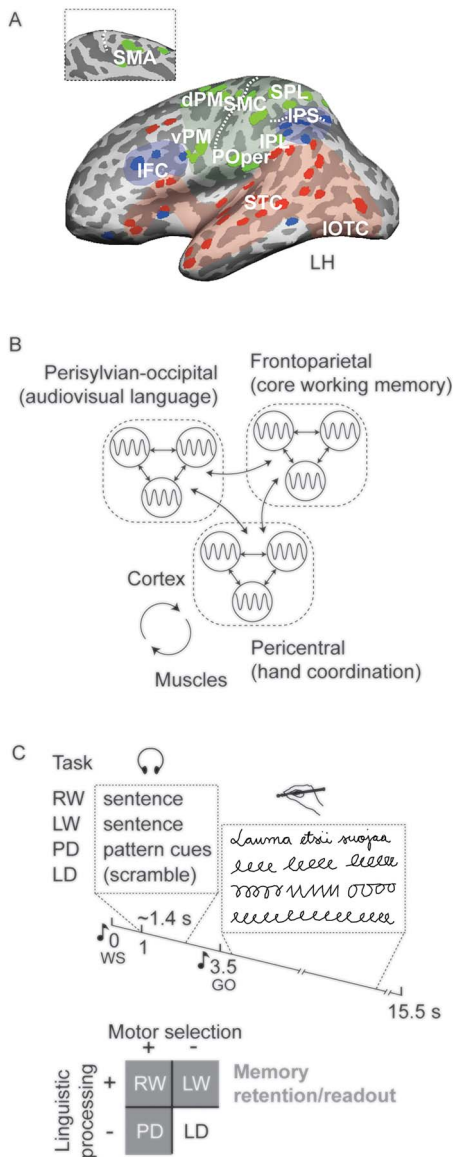
Figure 1. Hypothesized cortical system and experimental paradigm. (A) Estimation of the pericentral (green shade), frontoparietal (blue) and perisylvian-occipital (red) divisions of the cortex postulated to support handwriting in the left hemisphere (inset displays the dorsal medial view). Colored dots indicate the reference points derived from neuroimaging literature (as cited in the Methods). Dashed lines indicate the central and intraparietal sulci. dPM; IFC, inferior frontal cortex; IOTC, inferior occipitotemporal cortex; IPL, inferior parietal lobe; IPS, intraparietal sulcus; POper, parietal operculum; SMA; SMC, primary sensorimotor cortex; SPL, superior parietal lobe; STC, superior temporal cortex; vPM. (B) Schematic illustration of the hypothetical network system for handwriting consisting of the pericentral (hand coordination), frontoparietal (core working memory), and perisylvian-occipital (audiovisual language) subsystems. Nodal regions (circles) interact through coherent signaling (bidirectional arrows) within and between the subsystems. The pericentral module forms a control loop with the arm musculature. (C) In a delayed dictation-to-writing/audio cue-to-movement paradigm, the subjects first memorized sentences or auditory pattern cues and, right after, produced corresponding movements. The tasks included RW; LW; PD; and repetitive LD where nonsense scramble stimuli did not offer guidance for the movement. Timeline of a single experimental trial is presented under the task descriptions (WS, warning signal; GO, signal for starting the movement). (An example Finnish sentence [in RW] translates as "The herd seeks shelter".) The emphasis of task-associated motor and cognitive processes in each task is depicted below.

of memorized sentences or movement cues vs. noninstructed production in the LD task; Fig. 1C, see inset below).

We assumed that the studied task variants had a shared neural basis of task-relevant functional regions (e.g., Yuan and Brown 2015; Planton et al. 2017). Here, the first aim was to characterize task-sensitive modulation of common functional connections in that cortical network. The corticocortical connections-of-interest (COIs), determined as an average across the different task variants, were obtained with a data-driven MEG approach that estimates long-range interregional coherence [Dynamic Imaging of Coherent Sources (DICS); (Gross et al. 2001)]. The corticocortical COI estimation was complemented by mapping of coherence between the cortex and arm muscle activity. While linear coherence mapping was chosen as a robust tool for identification of COIs (Gross et al. 2001; Kujala et al. 2008; van Vliet et al. 2018), the subsequent quantification of task-dependent modulation of phase coupling between the nodal time series was done using the phase synchronization index (SI; Tass et al. 1998), a more sensitive metric to also capture nonlinear interactions of noisy neural oscillators (cf. e.g., Gross et al. 2002). To determine task-sensitivity as defined here, phase synchronization was contrasted between the task variants in each shared COI. A relatively stronger synchronization for one task than another was taken to indicate functional significance of a connection, associated with the specific differences in task features (Fig. 1C below). The second aim of the study was to compare how the changes in corticocortical phase synchrony relate to the postulated large-scale, modular system (Fig. 1A). The identified nodes were assigned to functio-anatomical subsystems whose spatial distribution was estimated with stereotaxic information from earlier literature. We expected that contrasts in motor task features would reveal interactions involving the pericentral subsystem, and linguistic content would engage the perisylvian-occipital subsystem, whereas cognitive and memory-related demands should highlight the frontoparietal subsystem.

Materials and Methods

Subjects and Tasks

Ten Finnish-speaking subjects (5 females; average age 29 years, range 20–40 years; one Finnish-Swedish bilingual) participated in the study. All the participants were right-handed (Edinburgh laterality index ≥80), and they reported frequently using handwriting for short notes. The participants gave their informed consent. The experiment was performed with a prior approval of the Helsinki and Uusimaa Hospital District Ethics committee (#9–49/2000).

The experiment included four variants of a handwriting task that used a delayed dictation-to-writing/audio cue-to-movement paradigm (Fig. 1C). The different task variants were performed in separate fifty-trial blocks. Each single trial comprised a warning signal (50-ms sine tone; 0.75-kHz) and a subsequent 1-s wait period, followed by the task-specific sentence/audio cue stimulus (mono sound, duration ∼1.4 s; 0.5–5-kHz; mean intensities equated). A go signal prompted the start of the movement (50-ms sine tone; 1 kHz), constantly at 3.5 s after the warning cue (∼1 s from the end of sentence/audio cue stimulus). A 12-s time interval was reserved for performance (total trial duration 15.5 s).

In real handwriting (RW), the subjects heard sentences and subsequently wrote them in their habitual normal lettering. A

new three-word sentence was presented in each of the 50 trials. The Finnish written language has a near perfect phoneme-to-grapheme correspondence and, therefore, the phonemic content of the heard sentences related highly regularly to the written patterns (the sentences were composed of 16–18 phonemes/letters; mean lengths of the 1st, 2nd, and 3rd word were 4, 6, and 7 phonemes/letters, respectively). All the sentences were semantically plausible, and they always started with a noun-verb pair followed either by a noun, verb, adjective, or adverb (e.g.,"Lintu laulaa puussa" [Engl. transl."A bird sings in the tree"]; "Kynä pitää teroittaa" ["The pencil must be sharpened"]; "Kala on terveellistä" ["Fish is healthy"]; "Into laantuu kohta" ["The enthusiasm dampens soon"]).

The loop writing (LW) task was a kinetically simplified version of RW where participants wrote heard sentences using a series of upcurved loops to represent words instead of the normal handwriting pattern. The production of loop patterns has been utilized in writing research as a rudimentary counterpart of handwriting (Thomassen and Meulenbroek 1998; Segal and Petrides 2012). While putting less demand on motor selection (cf., e.g., Schönle et al. 1986; Diedrichsen and Kornysheva 2015), the LW task was essentially similar to the RW: the subjects memorized heard sentences and thought they were writing them while producing only the loop series. In the LW task, the subjects were presented with a unique set of 50 three-word sentences (composed of 16–18 phonemes/letters; mean lengths of the 1st, 2nd, and 3rd word were 4, 6, and 6 phonemes/letters). The word frequencies did not differ between the RW and LW task sentences [Mann-Whitney test, $U(299) = 10\,714.5$, $P = 0.476$, n.s.; Finnish PAROLE Corpus (University of Helsinki, 1998)], nor did the distribution of phonemes ($\chi^2(17) = 9.34$, $P = 0.92$, n.s.; excluding categories "g", "d" and "ö" with <5 entries per task). Three series of loops were produced to represent each word of a sentence. While the phonology of sentences was not mapped into produced letters, the words of the sentence still guided the movement in a sense that they framed the produced loop series, as the subjects imagined writing with them. Fluent, intuitive performance without counting letters was emphasized. Yet, the subjects were encouraged to engage in imaginary writing and take time with each word; a pair of loops to tick off words was not accepted as valid performance.

Pattern drawing (PD) task according to memorized auditory cues served as a simple nonlinguistic analog of handwriting. The PD task was deliberately simpler than the overlearned RW (variation of series of patterns vs. individual letters) to maintain fluency of production at similar levels. Three distinct auditory cues were constructed: they were 0.5–5-kHz white noise signals (speech sounds filtered to the same band) that differed in their amplitude profile (either one, three, or nine Gaussian segments), with a duration of 0.47 s to approximate the length of words. The subjects were trained to associate these cues with three different movement patterns (saw-edges, downcurved loops, and connected circles). Learning of these audiomotor associations was individually followed, and all the subjects managed to acquire them. In each trial, three consecutive cues were presented in a varied order and different combinations: there are 24 possible permutations for three items, excluding those where the same item is repeated three times. These permutations were used twice (plus two randomly picked permutations for a third time) to form a 50-trial block. In each trial, the subjects were asked to produce a short series of movement patterns (aiming at five to six) in correspondence to the heard cues. Similarly to the sentences in the RW task, the auditory cues were retained in

working memory, and they instructed the selection of motor patterns for each produced series.

The loop drawing (LD) task consisted of monotonous, uninterrupted sequences of upcurved loops (filling the given writing space) that were produced in every trial. The LD task displayed conspicuous rhythmicity of movement. Unlike in the other conditions, the audio stimuli did not give any guidance for this performance, and the task constituted a simple baseline without invoking demands for memory retention and readout. Clips of unintelligible scrambled speech (each 50 RW sentence was segmented into 0.2-s samples, reversed and randomly assembled back together) replaced the guiding task-specific stimuli of the other tasks.

Recordings and Procedure

Cortical activity was recorded with an Elekta VectorView whole-head MEG device (Elekta Oy, Helsinki, Finland; 204 planar gradiometers organized as pairs of orthogonally oriented sensors, 102 magnetometers). The analysis used the planar gradiometers which pick up the maximal neuromagnetic signal above an active cortical site. The recorded signals were filtered to 0.03–200 Hz and sampled at 600 Hz. The MEG coordinate system was aligned with the individual magnetic resonance images (MRIs) (MRIs; 3 T General Electric Signa system, Milwaukee, WI, USA) by attaching four Head Position Indicator (HPI) coils to the scalp. The location of these coils was determined by energizing them before MEG data collection. This information was aligned with anatomical landmarks using a 3D digitizer system (Isotrak 3S1002, Polhemus Navigation Science, Colchester, VT) and, after the measurements, with the MRIs.

Electromyography (EMG) was recorded and monitored, simultaneously with MEG, from the right palm (*pollicis*), forearm (*e. carpi; f. digitorum*), shoulder (*deltoid*), and upper back (*infraspinatus*) muscles using bipolar surface electrodes. The analysis focused on the forearm (*e. carpi*) muscle which showed salient rhythmicity for the present movement tasks and whose activity has been previously shown to contain information related to handwriting patterns (Linderman et al. 2009). Eye movements and blinks were monitored with electrooculography (EOG).

During the MEG/EMG measurements, the subjects were seated under the MEG helmet. Auditory stimulation was presented binaurally through plastic tubes and intracanal earpieces at a comfortable listening level. The subjects performed the graphical tasks with their right hand using a cotton-tipped plastic stylus. This left no trace on a tilted panel with low-friction surface (width 16 cm, height 12 cm). The visual feedback of the writing performance was obstructed with a panel placed over the subject's forearms. The subjects stared at a given fixation point on the opposite wall (a cross with ∼1° visual angle), placed at approximately 21° elevation from the standard line of sight to counteract a potential head tilt towards the moving hand. Together, these procedures prevented efficiently eye movement artifacts in the MEG record, helped to retain an optimal orientation of the head within the MEG helmet, and emphasized hand somatosensory rather than visual feedback processing.

The subjects rehearsed all four tasks before the MEG measurement. To ensure vigilant performance, the experiment was conducted on 2 different days, on average 1 week apart. Each 50-trial task block (∼17 min) included four equally spaced 30-s intervals of rest (2 min rest in total). During the rest intervals, the

subjects were instructed to relax with their eyes open, holding the stylus and without moving. The task blocks were presented in a pseudorandomized order. The one exception to this rule was that the PD task was always presented on the second day. This arrangement allowed two premeasurement training sessions for this task and helped the subjects to become attuned with the measurement protocol before performing this newly learned task.

Half of the subjects ($n = 5$) additionally gave samples of their spontaneous performance in LD and RW before the MEG measurements. Here, EMG signals and graphical traces (on paper) were collected simultaneously to determine the relationship between the muscle rhythmicity and rate of graphical production.

Analysis of Movement Time Windows and Frequency-Bands-of-Interest

The EMG signals were high-pass filtered (>10 Hz) and rectified in order to highlight the envelope of muscle activity bursts. Movement onset and offset times were collected individually by setting a threshold value to distinguish EMG signal from the baseline noise (on average 43% $\pm$ 6 SD of the maximum value in the mean EMG trace). An in-house algorithm searched, trial-by-trial, for the first threshold crossing to collect the onset time and for the subsequent crossing below the threshold (for at least 0.2 s) to collect the offset time. The MEG analysis was focused on the consistent, continuous interval of movement production in each individual: first, the mean duration of movements across trials was determined for each task. Second, the minimum of these durations was selected and an interval of 1 s further subtracted from it. The analysis was restricted to this time window for every trial of every task. This window was centered, trial-by-trial, at the midpoint of movement or, if necessary, positioned so that it started at least 0.5 s after the go signal. In this way, approximately 5 min of data were collected for each task, per each subject.

The MEG signals were preprocessed with the temporal Signal Space Separation (tSSS) method to suppress artifacts arising outside the head space (Taulu and Simola 2006). Principal components (PCs) related to blinks and heart artifacts were removed as an extra precaution. The selection of frequency-bands-of-interest for the analysis of corticocortical interaction utilized information from the EMG-MEG coherence spectra, referenced to e. carpi muscle signal and the sensor-to-sensor MEG coherence spectra, quantified between sensors more than 10 cm apart, for each subject and task. The choice was guided by reference frequency bands: the delta/theta band, 1–8 Hz; low-alpha, 8–10 Hz; high-alpha, 10–12 Hz; low-beta, 13–19 Hz; high-beta, 20–30 Hz; low-gamma, 30–60 Hz; and high-gamma, 60–90 Hz [median band limits collected from the literature (von Stein and Sarnthein 2000; Buzsaki and Draguhn 2004; Wang 2010; Crone et al. 2011; Engel et al. 2013; Singer 2013; Babiloni et al. 2014; Cannon et al. 2014; Womelsdorf et al. 2014)]. At the frequency range where salient narrow-band spectral components were consistently distinguished (here < 25 Hz), the reference band limits were individually adjusted to incorporate the local maxima at a certain band and align with the surrounding minima found in each subject's data. The MEG-MEG coherence data were used in the alpha and beta bands. The delta/theta band showed generally a flatter profile in the MEG-MEG coherence spectra. Therefore, the EMG-MEG coherence data were used for the low-frequency band selection. This approach

also emphasizes the linkage of delta/theta frequencies to motor production (cf. Churchland et al. 2012; Hall et al. 2014). Before visualization, the spectra were normalized within each subject to the mean level in the 1–90 Hz frequency range across tasks in order to compensate for interindividual variation in the overall coherence level.

Mapping of COIs

The DICS mapping of all-to-all corticocortical coherence (Gross et al. 2001; Kujala et al. 2008) was used to identify, in a computationally tractable way, an unbiased set of COIs for subsequent evaluation of task-sensitive modulation of phase synchrony. Corticomuscular coherence was also mapped using DICS spatial filters. The DICS method is based on cross-spectral density matrices (CSDs) that represent linear dependencies of oscillatory signal components between the MEG sensors and between the MEG sensors and the EMG signal. Here, CSDs were calculated for each task as well as rest data with Welch's averaged periodogram method (Hanning 1024-point FFT-windows; 0.6 Hz resolution; 75% window overlap). Subsequently, the CSD data were projected individually into corticocortical estimates in the brain space with the DICS spatial filter. We focused on detection of long-range coherent connections, with the minimum distance set to 35 mm [taken the resolution of ∼2 cm of DICS mapping (Liljeström et al. 2005), the distance criterion can be reasonably set at >3–4 cm (e.g., Liljeström et al. 2015; Saarinen et al. 2015)]. The field spread inherent to electromagnetic field prevents reliable estimation of short-range coherence. The field spread varies across brain regions, and the true extent of the smoothness of the MEG estimates is further affected by the local power levels (Gross et al. 2003; Schoffelen and Gross 2009). We therefore chose to use a single consensus distance criterion that eliminates the most severe field spread effects, combined with contrasting of only power-matched conditions to further minimize any remaining influence of field spread. Coherence estimation was based on numerical maximization of coherence for a discrete set of source-orientation combinations (50 regularly spaced orientations of current flow at both ends of a connection, spanning the tangential source space with respect to a sphere at the center of the brain; approach applied, e.g., in Saarinen et al. 2015). This implementation enhances sensitivity to true coherent sources even when their power levels are low; in contrast, using a single fixed orientation at each location may result in coherence estimates that are severely (and incorrectly) biased by distant high-power sources. The coherence estimation was performed separately within each hemisphere, as well as between the hemispheres using grids that were confined to the individual brain volumes based on anatomical MRIs. The grids were set to be spatially equivalent across subjects: the grid points with 6-mm spacing were first determined in the atlas brain and then elastically transformed into the individual brains (Schormann et al. 1996). This enabled group-level statistical estimates of coherence. The most anterior tip of the frontal cortex was excluded from the analysis due to its relatively poor sensor coverage. In the lead field calculations, individual single-layer spherical conductor models were used.

To identify an unbiased set of COIs, the coherence values individually averaged across the variants of handwriting task (task-mean; ∼20 min of data) were contrasted with the mean coherence values in the rest data (8 min of data; collected as part of the task sessions), separately for each frequency band

of interest. COIs were identified on the basis of elevated coherence for task performance (task-mean > rest; paired, one-tailed t-statistics, $P < 0.0005$, uncorrected). The shorter rest data set was considered sufficient for the comparison, as the stability of coherence estimation has been shown to increase asymptotically beyond 2–3 min of collected data (Gross et al. 2003); importantly, this choice spared the subjects from extra (rest) measurements. The $P < 0.0005$ threshold represented a tradeoff between avoiding both scarcity and saturation of the connectivity graphs. For the nodal coordinates of these candidate coherent connections, hierarchical clustering (Matlab clusterdata function; minimum of three connections) was performed using a weighted distance algorithm (across both end-points of the connections) with a 20-mm cut-off threshold (Euclidean distance criterion). This clustering merges the results into spatially focal bundles that are more likely to represent true interregional interactions than the more distributed patterns that may originate from field spread. Finally, the network nodes were determined, within spectral subranges (low corresponding to the delta-to-alpha range; mid to beta; high to gamma), by spatially clustering the end-points of the coherent connection bundles (within 20 mm from each other) and by taking the mean cluster coordinates to represent the particular nodal region (see Results). The spatial clustering was also applied to significant cortico-muscular coherence results (paired, one-tailed t-statistics, task-mean > rest data, $P < 0.0005$) to identify the cortical areas that consistently cohered with the muscle activity. Power difference at each MEG sensor was tested for the studied frequencies (task-mean > rest data/between tasks; paired, one/two-tailed t-statistics, $P < 0.05$; false discovery rate corrected) in order to alleviate the risk of coherence estimates being affected by field spread.

Quantification of Task-Sensitive Modulation of Phase Coupling

The time series of activity at the COI endpoints were estimated for each subject with the DICS spatial filter, separately for each frequency-band-of-interest. Task-sensitive modulation of phase synchrony was then estimated for the COI time series using an entropy-based SI (Tass et al. 1998). The SI values of the task variants (RW, LW, PW, and LD; each ∼ 5 min of data) were contrasted against each other, pair-wise, with group-level significance evaluated using nonparametric permutation testing (Nichols and Holmes 2002): The original paired, two-tailed t-statistics were first calculated for the SI values in all coherent connections. Subsequently, the individual SI values of the two tasks were permuted in all possible combinations (1024 possible permutations for 10 subjects). At each permutation, t-statistics was calculated and the maximum t-score across the connections was stored, resulting in a distribution of 1024 t-values across permutations. The original t-values were then compared with this distribution, and t-values exceeding the 95% threshold were considered to represent a significant task-sensitive modulation.

Module Assignment of Network Nodes

We hypothesized that the neurocognitive system mediating handwriting would be composed of pericentral (hand coordination), frontoparietal (core working memory) and perisylvian-occipital (audiovisual language) subsystems, located primarily in the left hemisphere. These subsystems (Fig. 1A,B) were spatially estimated with the help of functional reference points

[MNI coordinates, or Talairach coordinates converted into MNI space, (Lacadie et al. 2008)] derived from previous, independent neuroimaging data (10 meta-analyses using positron emission tomography or functional MRI data; one fMRI connectivity study). In Figure 1A, this set of reference points was transformed into an individual cortical space (Schormann et al. 1996) for visualization.

For the pericentral subsystem, reference points were first collected from two meta-analyses on cortical substrates of writing (Purcell et al. 2011; Planton et al. 2013), which identified the component that relates most prominently to motor aspects of the task (i.e., "peripheral", "linguistic/input controlled" component). To render the set more inclusive and generally representative of hand motor coordination, the collected reference points were supplemented with points from meta-analyses that identified cortical substrates of simple finger tapping (Witt et al. 2008), hand motor function in young adults (Turesky et al. 2016), right-handed motor learning (Hardwick et al. 2013), object manipulation (Chouinard and Paus 2006), and action representation in tool use (Ishibashi et al. 2016). Altogether, 29 reference points were compiled in the central sensorimotor and adjacent frontal and parietal regions (thus label "pericentral"), and they faithfully covered the regions of the Human Motor Area Template (Mayka et al. 2006).

The Purcell et al. meta-analysis (Purcell et al. 2011) distinguishes the "peripheral" motor component from a "central" (cognitive and linguistic) component of written language processing that involves regions in the temporal, temporo-occipital, frontal, and parietal cortices. This central component overlaps with the cortical representation consistently described for language tasks (Vigneau et al. 2006), including regions reported in a seminal meta-analysis on semantic language tasks (Binder et al. 2009). Indeed, the cognitive architecture supporting writing has been thought to center on semantic processes (Purcell et al. 2011). Using the regions of the Binder et al. report (Binder et al. 2009) as nodes, a graph theoretical analysis of fMRI connectivity has uncovered a segregation of these regions into modules labeled as frontoparietal, perisylvian, and default mode networks (Xu et al. 2016). These network nodes were used here as reference points for the frontoparietal and perisylvian-occipital subsystems; the coordinates of the default mode network were also collected (18 points). The reference points from Xu et al. analysis (Xu et al. 2016) were supplemented, for the frontoparietal subsystem, with points taken from a meta-analysis on core cortical components of working memory function [across different types of tasks (Rottschy et al. 2012); altogether 14 points] and, for the perisylvian-occipital subsystem, with points combined from meta-analyses of reading [regions linked with early visual and prelexical processing of written forms (Jobard et al. 2003)] and of audiovisual processing of spoken language [for congruent auditory and visual signals (Erickson et al. 2014); altogether 33 points]. The reference points based on hemodynamic connectivity showed a marked overlap with those based on the meta-analyses of task-related cortical activation, but the task-related data further extended the reference set of the perisylvian-occipital subsystem to the occipitotemporal cortex.

Quantitative assignment of nodal regions found in the present data to these three estimated functional subsystems was based on the spatial proximity of a node to a reference cortical location described above. Taken the approximately 10–20 mm spatial resolution of MEG (Liljeström et al. 2005), a node closer than 15 mm in the MNI space to a reference point was assigned to that functional subsystem.
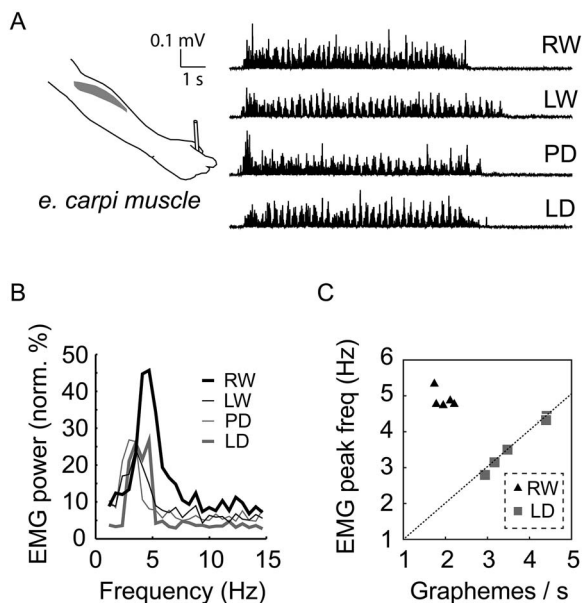
Figure 2. Arm muscle activity during movement sequences. (*A*) Example EMG traces (in a single subject) for each variant of the handwriting task. (*B*) Normalized mean EMG spectra (*n* = 10) for each variant of handwriting task (recorded from e. carpi arm muscle; high-passed, rectified signals; spectra normalized individually to the maximum value across tasks before averaging across subjects). (*C*) Individual EMG peak frequencies as a function of grapheme rate per second for letters (RW task) and loops (LD task) in spontaneous production (subset of *n* = 5).

Results

Muscle Rhythmicity Settles at 2–5 Hz for the Variants of Handwriting

All variants of the handwriting task (Fig. 1C) were associated with sustained arm muscle activity that featured rhythmic bursts at approximately 2–5 Hz (see the fine-structure in EMG traces corresponding to the spectral peaks; Fig. 2A,B). Motor performance was similar between the task variants and across the trials of MEG measurements; however, the RW task displayed a slightly longer duration (1.0 s), higher rate (1.1 Hz) and, on average, higher EMG amplitude at the beginning of the measurement session (see Supplementary Fig. S1). The salient muscle rhythmicity was linked with graphical performance (Fig. 2C): When the extreme conditions of simple LD and complex RW were examined in a separate test on five participants, the peak frequency of the EMG spectrum directly corresponded to the rate of simple LD (cross-subject average rate 3.5 ± 0.6 Hz [mean $\pm$ SD]). In contrast, for RW, the EMG peaks consistently clustered near 5 Hz (4.9 ± 0.3 Hz) while the rate of letter production settled at approximately 2 Hz (1.9 ± 0.3 Hz) (analogously to the syllable and word rates of speech, for example, Ruspantini et al. 2012). Thus, unlike simple loops, an average letter consistently associates with 2–3 muscle activity bursts reflecting strokes needed for pattern construction.

Data-Driven Mapping of Corticocortical Coherence During Motor Performance Provides COIs for Characterizing Phase Synchrony

The EMG-MEG and MEG-MEG coherence spectra (Fig. 3A), calculated across individuals and sensors, emphasized different
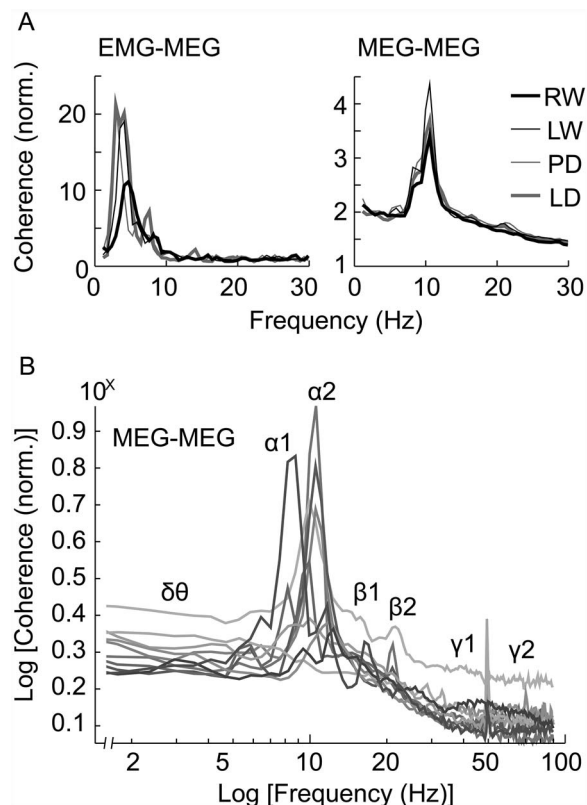
Figure 3. Coherent neural frequencies. (*A*) Normalized mean coherence spectra (*n* = 10) between the arm muscle and the MEG sensors located above the SMC (EMG-MEG; above) and the mean coherence spectra between pairs of left-sided MEG sensors at a minimum distance of 10 cm (MEG-MEG; below). For task abbreviations, see the Introduction. (*B*) The log-log plot of mean MEG-MEG coherence spectra for each subject (*n* = 10) averaged across the tasks. The specific frequencies of interest are indicated with Greek lettering.

frequency components in continuous motor production (reaching maximum at ~2–5 vs. 10 Hz, respectively). Figure 3B displays the individual patterns of MEG-MEG coherence, calculated across tasks and sensors. The low- and mid-frequency ranges (below ~25 Hz) manifested spectral peaks (Fig. 3A,B). In order to maximize representativeness, this spectral information was used to individually adjust the literature-derived reference band limits (see Methods). The delta/theta band was determined on the basis of the salient component in the EMG-MEG spectra, and the alpha and beta bands were determined from the MEG-MEG spectra. On average, 1.8 Hz ($\pm$1.6 Hz SD) adjustments were made to the reference limits. The group-average band limits were, at the low spectral range, 2–5 Hz for the delta/theta band ($\delta\theta$) and 7–10/10–13 Hz for the low/high-alpha band ($\alpha1/\alpha2$). At the midrange, the band limits were 14–18/18–24 Hz for the low/high-beta band ($\beta1/\beta2$). As there were less distinctive spectral features within the high spectral range, fixed limits were used across the individuals for the low/high-gamma band ($\gamma1/\gamma2$; 30–45/60–90 Hz; avoiding the power-line artifact at 50 Hz).

The corticocortical estimates of task-related long-range coherence were mapped within each hemisphere and between hemispheres, separately for the low, mid, and high spectral ranges (task-mean > rest data, pooled across the variants of handwriting task and frequency-bands-of-interest; one-tailed t-statistics, bundles of at least 3 uncorrected connections

Table 1 Corticocortical connections showing task-sensitive modulation of synchrony for the variants of handwriting

Connected regions	MNI (x,y,z; x,y,z)	Effect	Band	Mean SI (Δ%[a])
Left hemisphere				
a. IFC—IPS	(−50, 15, 20; −29, −47, 39)	RW > LD	$\delta\theta$	0.190 (4)
b. vPM—dPM	(−43, 4, 33; −16, −13, 64)	LD > PD/RW	$\alpha1$	0.207 (7/4)
c. STS—IOC	(−48, −38, −2; −28, −78, −6)	LW > LD	$\alpha1$	0.210 (7)
d. TPOj—POC	(−41, −59, 15; −20, −81, 43)	LD > RW	$\alpha2$	0.178 (7)
e. SMC—SMA	(−45, −19, 58; −13, 8, 50)	RW > LW	$\beta1$	0.271 (51)
f. IPL—dPM[b]	(−49, −48, 48; −28, −16, 68)	RW > LD	$\beta2$	0.178 (28)
g. IPL—SMC[b]	(−49, −48, 48; −41, −14, 55)			
h. IPoCS—SPoCS	(−51, −24, 34; −27, −41, 58)	PD > LW	$\beta2$	0.128 (13)
i. IPL—POper	(−50, −48, 49; −63, −14, 27)	PD > LD	$\gamma1$	0.107 (50)
Right hemisphere [c]				
j. POper—dPM	(63, −16, 16; 13, −8, 58)	PD > LD	$\delta\theta$	0.214 (12)
k. POper—SFC	(48, −25, 21; 29, 6, 46)	PD > LW	$\beta2$	0.214 (27)
Across hemispheres				
l. lSPL—rSPL	(−20, −64, 67; 21, −45, 57)	PD > RW	$\alpha1$	0.220 (8)
m. lvPM—rSMA	(−59, −1, 31; 5, −11, 51)	LD > LW	$\alpha2$	0.173 (3)
n. lSMC—rSMA	(−61, −11, 24; 5, −11, 51)	LD > LW	$\alpha2$	0.176 (3)
o. lMPL—rSMA	(−9, −60, 46; 4, −20, 67)	LW > PD	$\alpha2$	0.180 (4)
p. lSFC—rSMC	(−18, −3, 60; 44, −19, 55)	LD > PD	$\beta1$	0.146 (10)
q. lSPL—rdPM	(−19, −46, 64; 38, −15, 68)	PD > LD	$\gamma2$	0.049 (36)

[a] Δ%, percentual change of the mean SI level between the contrasting tasks.
[b] These connections were treated as representing one functional connection.
[c] One task-sensitive connection (between the right occipital [MNI 7, −78, 30] and anterior temporal [52, 15, −30] cortices, PD > LD) was excluded from the results, as its SI values (mean 0.05 ± 0.002 SD) remained under the 5th percentile of the SI distribution of the other connections (mean 0.18 ± 0.07 SD).
d/vPM; IFC, inferior frontal cortex; IOC, inferior occipital cortex; IPL, inferior parietal lobe; IPoCS, inferior postcentral sulcus; IPS, intraparietal sulcus; MPL, medial parietal lobe; POC, parieto-occipital cortex; POper, parietal operculum; SFC, superior frontal cortex; SMA; SMC, primary sensorimotor cortex; SPL, superior parietal lobe; SPoCS, superior postcentral sulcus; STS, superior temporal sulcus; TPOj and l/r, left/right hemisphere.

[P < 0.0005] qualified as positive connection at each band; spatial clustering at the end points). These connectivity patterns (Fig. 4A) provided data-driven COIs for subsequent characterization of task-sensitive modulation of phase synchrony. No parallelly occurring power modulation (task-mean > rest data) was found at the studied frequencies at any MEG sensor (paired, one-tailed t-statistics, P < 0.05; false discovery rate corrected), nor was there power modulation between the task variants (paired, two-tailed t-statistics, P < 0.05; false discovery rate corrected). The coherence mapping was robust against changes of bundle size and distance criterion in spatial clustering (Fig. 4B). The nodal regions found in the all-to-all corticocortical mapping extended well beyond the regions that were identified with corticomuscular coherence that is linked most directly to motor performance (Fig. 4C).

Task-Sensitive Modulation of Corticocortical Phase Synchronization Reveals Distinct Functional Elements Supporting the Variants of Handwriting

Figure 5 illustrates the corticocortical elements manifesting task-sensitive modulation of phase synchrony for the different variants of the handwriting task (Fig. 1C). For each COI derived from the coherence mapping within and across the hemispheres, SI values were calculated for the task variants, and the tasks were contrasted against each other (maximum-statistics permutation testing based on paired, two-tailed t-statistics, 95% threshold for significance). Table 1 summarizes these task-modulated connections (a–q), excluding one extremely weak connection in the right hemisphere.

Out of 17 significant connections, nine were located within the left hemisphere (Fig. 5A). At low frequencies, there were diverse task effects that represented subtle changes (4–7%) in cortical population synchrony (Table 1, left hemisphere). The delta/theta synchronization between the inferofrontal and intraparietal cortices (connection a) was stronger for the RW than for the LD task. In contrast, the low-alpha synchronization between the dPM and vPM (b) was stronger for the repetitive LD than for the motorically more varied PD and RW tasks. At the same band, the superotemporal and infero-occipital cortices (c) synchronized more for the LW than LD task. Moreover, synchronization at the high-alpha band was stronger for the LD than real writing task between the temporo-parieto-occipital junction (TPOj; lower part of the angular region) and the parieto-occipital cortex (d).

The mid-to-high frequency range showed relatively greater changes in phase synchrony (13–51%) than the lower frequencies, and the stronger synchronization always favored a more varied motor task in comparison with a simpler variant. The most prominent modulation among all task-sensitive effects was the stronger low-beta synchronization for the RW than for the LW task between the left-hemisphere hand SMC and the (pre−/) supplementary motor cortex (e). At the high-beta band, the inferior parietal cortex (near the intraparietal sulcus) and two nodes in the premotor/ precentral cortex (f, g) synchronized more strongly for the RW than LD task. At the same band, the inferior and superior postcentral regions (h) synchronized more for the PD than LW task. At the low-gamma band, there was stronger synchronization between the left inferior parietal and parieto-opercular cortices (i) for the PD than LD task.

Within the right hemisphere (Fig. 5A and Table 1, right hemisphere), two connections highlighted the PD task: the parieto-opercular cortex showed task-sensitive synchronization with the premotor cortex at the delta/theta band (j) and with the
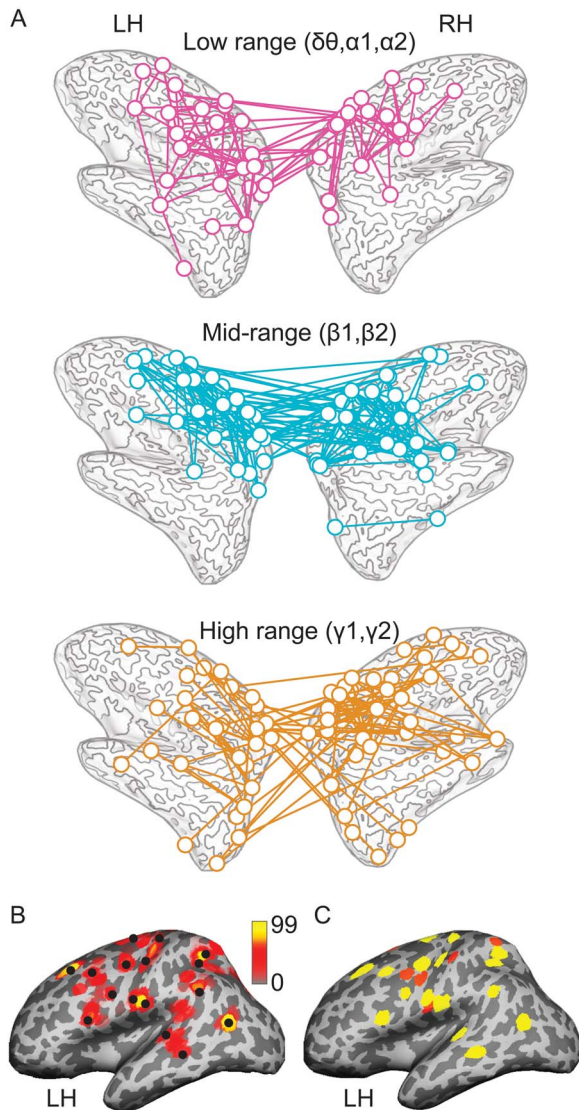
Figure 4. Mapping of the COIs. (A) Networks comprised of the coherent COI mapped at the low, mid, and high spectral ranges within and between the left and right hemispheres. (B) Robustness of identifying the coherent nodes (exemplified at low frequencies in the left hemisphere) when the clustering parameters of mapping were varied (bundle sizes 2–10; distance criterion 15–25 mm; rendering a total of 99 parameter combinations). The color-coding represents the number of parameter combinations that revealed a specific node. Black dots indicate the nodes selected for the present mapping (with bundle size of 3 and distance criterion 20 mm). (C) The nodes of corticocortical coherence (yellow) at the low spectral range superimposed with the regions (red) showing corticomuscular coherence (at ∼2–5 Hz).

superior frontal cortex at the high-beta band (k). Across hemispheres, there were six task-modulated connections (Fig. 5B and Table 1, Across hemispheres): The left and right superior parietal cortices showed stronger low-alpha synchrony for the PD task than for the handwriting task (l). At the high-alpha band, the left ventrocentral regions (m, n) synchronized more strongly with the right SMA region in the LD than LW task, whereas the left medioparietal cortex synchronized more strongly with the right superior frontal cortex in the LW than in the PD task (o). The left superior frontal region showed stronger low-beta

synchrony with the right SMC for the LD task when compared with PD (p). By contrast, there was weak high-gamma synchrony between the left paracentral and right premotor/hand sensorimotor regions (q), which was stronger for the pattern than LD task.

Here, we applied SI to quantify the task-sensitive modulation of phase synchrony within the identified networks. We also tested how well the SI-based modulations would have been detected with coherence that captures the linear aspects of the same phenomena. Out of the 17 connections that showed significant modulations with SI, 12 reached significance also with coherence. The finding suggests that SI is a more sensitive measure for capturing fine-grained modulations of phase synchrony than coherence. This results from the increased variance of coherence (due to amplitude modulations) compared with SI (3.4 times higher level of SD/mean relationship for coherence than SI values in the identified connections) and the insensitivity of coherence to nonlinear phase relationships.

The Nodes of Task-Modulated Synchrony Align with the Postulated Subsystems of the Handwriting Network

The cortical layout of the three postulated subsystems (pericentral, frontoparietal, and perisylvian-occipital; Fig. 1A) for handwriting was spatially estimated using 76 stereotactic reference points that have shown relevant functional sensitivity in previous literature (Fig. 6; cf. Methods). Out of the 18 nodes identified for task-modulated connectivity within the left hemisphere in the present study, 17 matched closely with one of the reference points (at the distance of 5–14 mm; criterion of < 15 mm distance in the MNI space). The one remaining node found a close match with a reference coordinate related to the so-called default mode system (distance 5 mm; gray). Task-sensitive connectivity (Table 1 and Fig. 5) was found within each subsystem (connections b, e, h within pericentral; a within frontoparietal; c within perisylvian-occipital) and between the pericentral and frontoparietal subsystems (f, g, i). The node found in the default mode system interacted with a node assigned to the perisylvian-occipital subsystem (d).

Discussion

The participants produced variants of a handwriting task that ranged from real and motorically simplified writing to sequential drawing of varied patterns and monotonous loops. When these variants with their specific motor, linguistic, and cognitive task demands were contrasted, we found that phase synchronization was modulated in a set of functional corticocortical connections. In the left hemisphere, a diverse pattern of task-sensitive modulation was observed for low-frequency synchrony (∼2–13 Hz) between nodal regions extending to the temporal and occipital cortices, whereas stronger phase synchrony in the beta-to-low-gamma range (∼13–45 Hz) was uniformly associated with the motorically more complex task variants and delimited to the central and frontoparietal connectivity. A few task-sensitive connections were also identified in the right hemisphere, as well as a number of connections across hemispheres, with none of them specifically highlighting the regular handwriting task. In correspondence to the hypothesized cortical network system (Fig. 1A,B), the task-modulated connections were found primarily within and between the pericentral (hand coordination) and frontoparietal (core working memory)
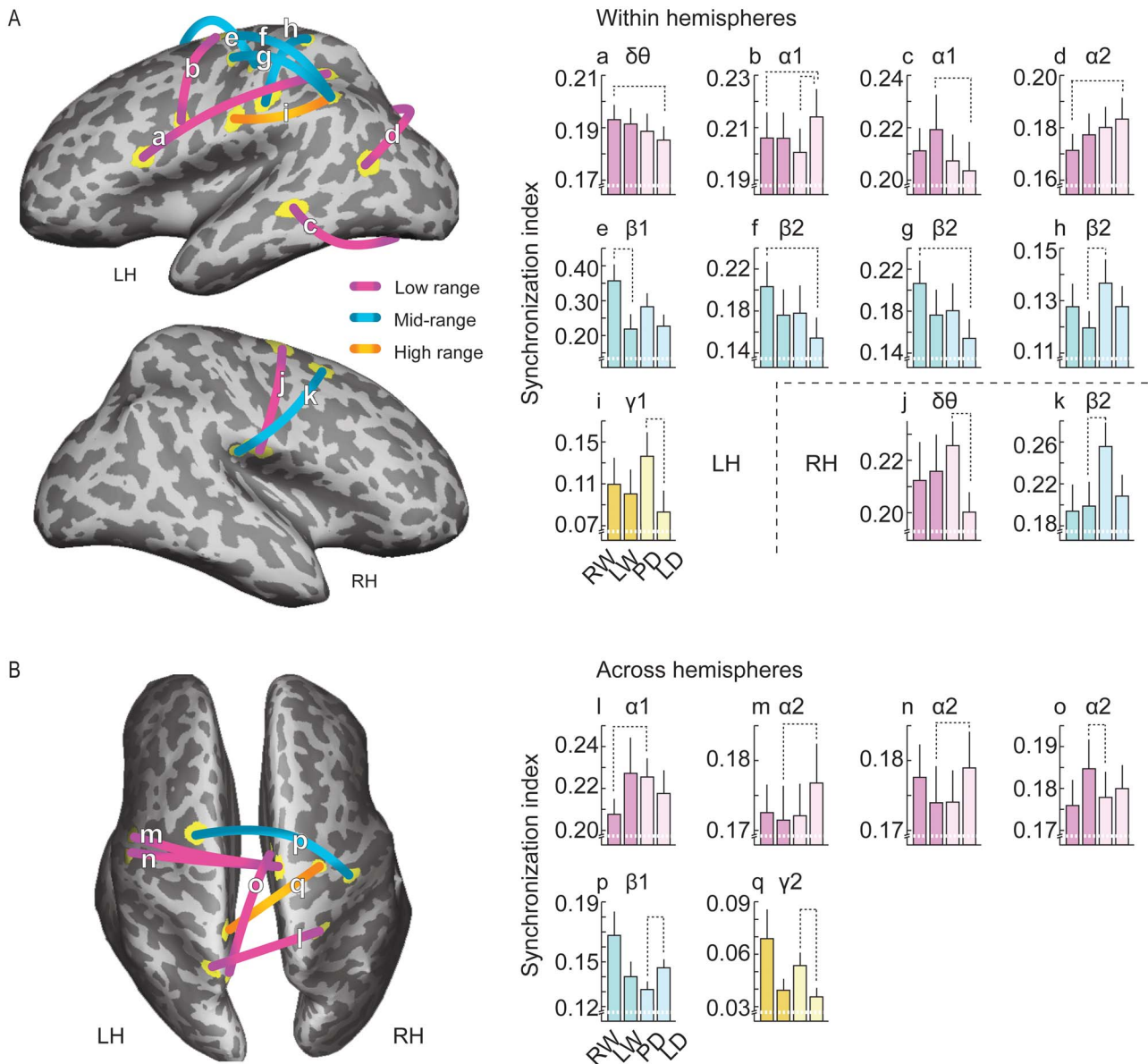
Figure 5. Task-sensitive corticocortical phase synchronization in the left and right hemispheres (A) and across the hemispheres (B). The cortical surface view illustrates the corticocortical connections (a–q), which showed modulated phase synchrony for the different variants of handwriting task (Fig. 1C). Color-coding refers to the spectral ranges. The bar graphs (below) show SI values (±SEM) for each connection. Task contrast (*n* = 10; maximum-statistics permutation testing based on t-statistics, 95% threshold) and the frequency band of the effect are indicated. Note the different ranges of y-axis values and the fact that permutation testing can highlight statistical differences that do not fully comply with the apparent differences in mean SI levels (see, e.g., connections p and q).

subsystems, and only a single connection was detected within the perisylvian-occipital (audiovisual language) subsystem.

Task-Sensitive Corticocortical Synchrony and the Postulated Subsystem Model

The identified left-hemispheric nodes of task-modulated interactions overlapped and aligned with the estimated spatial configuration of the postulated functio-anatomical subsystems (Fig. 1A,B). Task-sensitive modulation of interactions within each subsystem was observed at the delta/theta or low-alpha frequencies; beta-to-low-gamma band manifested task-sensitive modulation of synchrony within the pericentral

subsystem and from the pericentral subsystem to the frontoparietal subsystem. Indeed, the majority of the modulated interactions were found within and between the pericentral and frontoparietal subsystems (see the next section), suggesting that the task-sensitive adjustment of phase coupling mainly involved the interconnected regions coordinating motor output and mediating working memory processes that supported the to-be-produced movements (Fig. 1B).

Separate, functionally distinct low-alpha synchrony was observed within the perisylvian-occipital subsystem (connection c; Fig. 5). In previous perceptual studies, temporo-occipital interaction at the alpha band has been associated with written language and audiovisual processing (Kujala et al.
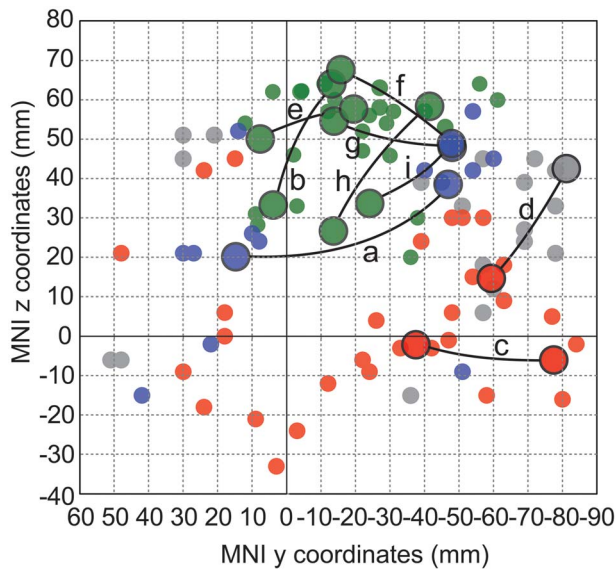
Figure 6. Assignment of the nodal regions to the postulated cortical subsystems. The plot (3-dimensional MNI data projected to the y-z plane) illustrates the nodes of the task-sensitive connections (larger connected circles) and the reference points (smaller circles) for the postulated subsystems that support handwriting (pericentral in green, frontoparietal in blue, and perisylvian-occipital in red; see Fig. 1A,B), and points representing the "default mode" system (gray). Each connection is labeled (a–i) as in Figure 5.

2007; Chandrasekaran and Ghazanfar 2009; Thorne et al. 2011). Here, with no direct visual stimulation, the effect of relatively stronger synchrony for the LW than LD task likely relates to the linguistic context of hand movements, as the motor demands were practically equivalent in the contrasted tasks. Notably, though, this connection showed only an intermediate level of synchronization for the RW task. This apparently counterintuitive finding may be interpreted in terms of the overlearned nature of real writing that presumably emphasized hand sensorimotor rather than audiovisual processing during production. It may be speculated that the present LW task promoted covert audiovisual processing in form of pronounced internal simulation of phonemes and letter forms of the sentences (or even, e.g., counting the letters, against instructions).

The posterior perisylvian cortex hypothetically interacts with the frontal and parietal regions in association with writing performance as part of the readout process of the verbal message to motor output (see discussion in Roux et al. 2014). Here, writing-sensitive phase synchronization from the perisylvian-occipital subsystem to the frontoparietal and/or pericentral subsystems was not detected, suggesting that this type of coupling may not play a notable and temporally sustained role in an on-going writing process [cf. transient interaction in oral word repetition (Flinker et al. 2015)]. While a relatively small number of participants, specific metrics of interaction and a nongenerative type of writing task may contribute to the negative finding, it is noteworthy that the perisylvian nodes have, indeed, not been the most consistently activated substrate of writing (cf. Planton et al. 2013).

Outside the subsystem model, a node assigned to the default mode system was coupled with the posterior perisylvian cortex (that also bordered the lateral "default mode" reference locations) and this synchrony at the high-alpha band favored the most monotonous task variant; this type of connection fits with the mediolateral connectivity of the default mode system that

has been linked with alpha-band activity (Capotosto et al. 2014) and with relative disengagement from externally oriented task performance (Fox et al. 2005; Raichle 2015).

Task-Sensitive Modulation of Corticocortical Synchrony for Handwriting Versus Loop Production

A similar set of cortical regions mediates writing and closely related motor tasks (Yuan and Brown 2015; Planton et al. 2017), and the present characterization provides insights into the task-sensitive modulation of the individual connections within a functional network formed by such regions. Here, the actual handwriting task showed stronger phase synchrony than the simple loop production variants in the left SMC-SMA, parieto-premotor, and parieto-frontal connections. This set of cortico-cortical elements can be interpreted to reflect different levels of cognitive-motor processing, despite their comparable functional sensitivity.

Within the putative precentral subsystem (Fig. 1A,B), the low-beta SMC-SMA coupling (connection e; Fig. 5) featured the most salient synchronization effect. As the contrasted tasks (RW > LW) differ in motor variability but not in linguistic content as such, this finding aligns with the pivotally motor-related role of these two cooperating regions (see Planton et al. 2013). Beta-band signaling and interareal coupling has been linked with SMC, SMA, and the associated subcortical nuclei (e.g., Salmelin et al. 1995; Gross et al. 2005; Oswal et al. 2016), and SMC-SMA interaction at these frequencies has shown sensitivity to complexity of finger movement sequences (Manganotti et al. 1998; Boenstrup et al. 2014). The present data extend these findings to stylus use and shows enhanced beta-coupling for complex rather than simple coordination of writing-related movements.

At the high-beta band, the parieto-premotor synchrony (connections f and g; Fig. 5) contrasted between the task variants with the most and least cognitive-motor demands (RW > LD). The observed corticocortical synchrony represented interaction between subsystems (frontoparietal–pericentral; Fig. 1B): the posterior parietal cortex can be viewed to harbor more abstract (or sensory-based) representations of intended movement (Hommel et al. 2001; Fuster 2004; Desmurget and Sirigu 2009; Roby-Brami et al. 2012), whereas the dPM/precentral region, critically associated with handwriting (Sugihara et al. 2006; Roux et al. 2009), seems to be more concretely involved in motor production and incorporate parietal influence (see Graziano 2016). Indeed, the cooperation between these two regions likely reflects cognitive-motor guidance of writing movements. In support of this view, previous studies have associated beta-band interaction between the premotor/precentral and parietal cortices with (transient) cognitive-motor tasks (Chung et al. 2017; Martínez-Vázquez and Gail 2018), possibly serving as a type of filter mechanism for task-relevant interregional neural processing (Antzoulatos and Miller 2016).

Between the intraparietal and inferior frontal nodes of the frontoparietal subsystem (connection a; Fig. 5), task-sensitive synchronization was found at the delta/theta band that links with motor performance but has also been associated with sustained neurocognitive processing in the frontoparietal cortex (e.g., Daitch et al. 2013; Szczepanski et al. 2014). While there were memory requirements in the LW and PD tasks (Fig. 1C), the combination of verbal memory retention and complex motor patterning of handwriting highlighted higher temporal accuracy of interregional coupling when compared with simple motor

patterning. Indeed, as core substrates for cognitive processing, activity of these regions has been related to both verbal memory maintenance and segmental processing of motor sequences (e.g., Wymbs et al. 2012; Bonhage et al. 2014). Thus, the task-sensitive frontoparietal synchrony seems to reflect stability of the cognitive frame that supports production of elaborate sequences.

In contrast, the left ventral and dorsal premotor cortices (connection b; Fig. 4) showed stronger low-alpha synchrony for the monotonous loop production than for either the varied PD or RW tasks. This frequency band of synchrony has prominently manifested in earlier characterization of corticocortical interactions during continuous motor production (Gross et al. 2002; Pollok et al. 2005; Butz et al. 2006), but the present effect may seem unexpected as the premotor cortical regions have been widely associated with complex rather than simple movements. Notably, though, the mutual interaction of the functionally distinct vPM and dPM cortices has remained largely unresolved (van Polanen and Davare 2015). Indeed, the present finding suggests relatively independent contributions from these regions in a complex motor task [note the particular role of dPM in handwriting (Sugihara et al. 2006; Roux et al. 2009)] or, conversely, that less motor variation leads to elevated low-frequency synchrony between them.

Furthermore, unlike other task variants, the PD task required mapping of newly acquired auditory cues to specific motor outputs. This may explain the enhanced beta-coupling of the left inferior and superior postcentral regions (connection h; Fig. 4; cf. Brovelli et al. 2004; Segal and Petrides 2012), which have been collectively linked with sensory and sensorimotor integration (e.g., Sepulcre et al. 2012; Rizzolatti and Sinigaglia 2016). The opercular regions that relate to secondary somatosensory processing (Hari and Forss 1999; Eickhoff et al. 2006) were also bilaterally involved in the synchronous connections that were enhanced for the newly acquired task. In the left hemisphere, the opercular-parietal synchrony at the low-gamma band (connection i; cf. Jensen et al. 2015) potentially associates with interregional processing of reafferent signals that update higher-order movement goals. The two right-hemispheric connections from the opercular region to the dorsal frontal cortex (connections j and k) may link with sensorimotor and attention-related processing (cf. Corbetta and Shulman 2002; Planton et al. 2013); the delta/theta and high-beta frequencies of these interactions could reflect spectrally distinct functions, such as bottom-up and top-down interactions (Bastos et al. 2015; Babapoor-Farrokhran et al. 2017).

Across the hemispheres, synchronous connections also emerged to highlight either the PD task (connections l and q) or simple loop production variants (m, n, o and p). Representing the latter type, there was a low-beta-band connection between the left superior frontal cortex and the right ipsilateral SMC (connection p), which may be compared with the left SMA–(contralateral) SMC connection (e) that favored RW. There were qualitative similarities in the mean SI profiles of these connections (Fig. 5A,B) but, importantly, the tested task-sensitive modulation differed between them, suggesting also functional differentiation. Moreover, a task-modulated connection was found between the right and left parietal cortices that synchronized, in the low-alpha band, more for the PD than handwriting task (l). This noteworthy effect is in line with the enhanced bilateral parietal involvement that has been previously reported for drawing in comparison with writing (cf. e.g., Potgieser et al. 2015).

Methodological Considerations

The present characterization of phase synchrony focused on long-range corticocortical connections that can be reliably determined from noninvasive electrophysiological recordings and on consistent connectivity patterns during unfolding production of the handwriting variants; unavoidably, this approach may overlook some local or transient interactions. The modulation of phase synchrony, as quantified between the task variants, allows relative characterization and does not determine if changes should be interpreted as elevations or suppressions of phase coupling with respect to some generic baseline. It should also be noted that we identified task-sensitive modulations of synchrony in the interregional connections shared by the different tasks and did not aim to determine spatially distinct task-specific network components as such levels of synchrony could not be directly compared between tasks. A rather small sample ($n = 10$) seemed sufficient for this characterization, in line with previous reports of coherence mapping during motor tasks (cf. Gross et al. 2002; Butz et al. 2006), but caution should be exercised particularly in interpreting negative findings. The present pattern of phase coupling relates to the specific writing conditions where the subjects did not have typical visual feedback; corticocortical interactions associated with the visual and oculomotor processes of writing warrant a separate examination.

Concluding Remarks

We found task-sensitive modulation of phase synchrony in the corticocortical elements that aligned with the hypothesized modular network of handwriting. Synchronies within and between the putative pericentral and frontoparietal subsystems were enhanced for regular handwriting, reflecting different processing levels of motor coordination, cognitive guidance of movement and working memory maintenance of cognitive frame; a separate enhancement of perisylvian-occipital synchrony was found when the endpoint of the writing task was a simplified output pattern. As a metric of population-level cortical dynamics, phase synchrony of interregional connections was shown here to reflect distinct cognitive-motor demands in production of movement sequences.

Supplementary Material

Supplementary material is available at *Cerebral Cortex* online.

Funding

Notes

References

Alexander MP, Friedman RB, Loverso F, Fischer RS. 1992. Lesion localization in phonological agraphia. *Brain Lang.* 43:83–95.

Antzoulatos EG, Miller EK. 2016. Synchronous beta rhythms of frontoparietal networks support only behaviorally relevant representations. *elife.* 5:e17822.

Babapoor-Farrokhran S, Vinck M, Womelsdorf T, Everling S. 2017. Theta and beta synchrony coordinate frontal eye fields and anterior cingulate cortex during sensorimotor mapping. *Nat Commun.* 8:13967.

Babiloni C, Del Percio C, Arendt-Nielsen L, Soricelli A, Romani GL, Rossini PM, Capotosto P. 2014. Cortical EEG alpha rhythms reflect task-specific somatosensory and motor interactions in humans. *Clin Neurophysiol.* 125:1936–1945.

Barbey AK, Colom R, Solomon J, Krueger F, Forbes C, Grafman J. 2012. An integrative architecture for general intelligence and executive function revealed by lesion mapping. *Brain.* 135:1154–1164.

Bastos AM, Vezoli J, Bosman CA, Schoffelen JM, Oostenveld R, Dowdall JR, De Weerd P, Kennedy H, Fries P. 2015. Visual areas exert feedforward and feedback influences through distinct frequency channels. *Neuron.* 85:390–401.

Bertolero MA, Yeo BT, D'Esposito M. 2015. The modular and integrative functional architecture of the human brain. *Proc Natl Acad Sci U S A.* 112:E6798–E6807.

Binder JR, Desai RH, Graves WW, Conant LL. 2009. Where is the semantic system? A critical review and meta-analysis of 120 functional neuroimaging studies. *Cereb Cortex.* 19:2767–2796.

Boenstrup M, Feldheim J, Heise K, Gerloff C, Hummel FC. 2014. The control of complex finger movements by directional information flow between mesial frontocentral areas and the primary motor cortex. *Eur J Neurosci.* 40:2888–2897.

Bonhage CE, Fiebach CJ, Bahlmann J, Mueller JL. 2014. Brain signature of working memory for sentence structure: enriched encoding and facilitated maintenance. *J Cogn Neurosci.* 26:1654–1671.

Bressler SL, Coppola R, Nakamura R. 1993. Episodic multiregional cortical coherence at multiple frequencies during visual task performance. *Nature.* 366:153–156.

Brovelli A, Ding M, Ledberg A, Chen Y, Nakamura R, Bressler SL. 2004. Beta oscillations in a large-scale sensorimotor cortical network: directional influences revealed by granger causality. *Proc Natl Acad Sci U S A.* 101:9849–9854.

Butz M, Timmermann L, Gross J, Pollok B, Dirks M, Hefter H, Schnitzler A. 2006. Oscillatory coupling in writing and writer's cramp. *J Physiol Paris.* 99:14–20.

Buzsaki G, Draguhn A. 2004. Neuronal oscillations in cortical networks. *Science.* 304:1926–1929.

Cannon J, McCarthy MM, Lee S, Lee J, Borgers C, Whittington MA, Kopell N. 2014. Neurosystems: brain rhythms and cognitive processing. *Eur J Neurosci.* 39:705–719.

Capotosto P, Babiloni C, Romani GL, Corbetta M. 2014. Resting-state modulation of alpha rhythms by interference with angular gyrus activity. *J Cogn Neurosci.* 26:107–119.

Chandrasekaran C, Ghazanfar AA. 2009. Different neural frequency bands integrate faces and voices differently in the superior temporal sulcus. *J Neurophysiol.* 101:773–788.

Chenoweth NA, Hayes JR. 2003. The inner voice in writing. *Writ Commun.* 20:99–118.

Cheyne D, Ferrari P. 2013. MEG studies of motor cortex gamma oscillations: evidence for a gamma "fingerprint" in the brain? *Front Hum Neurosci.* 7:575.

Chouinard PA, Paus T. 2006. The primary motor and premotor areas of the human cerebral cortex. *Neuroscientist.* 12:143–152.

Chung JW, Ofori E, Misra G, Hess CW, Vaillancourt DE. 2017. Beta-band activity and connectivity in sensorimotor and parietal cortex are important for accurate motor performance. *NeuroImage.* 144:164–173.

Churchland MM, Cunningham JP, Kaufman MT, Foster JD, Nuyujukian P, Ryu SI, Shenoy KV. 2012. Neural population dynamics during reaching. *Nature.* 487:51–56.

Colombo M. 2013. Moving forward (and beyond) the modularity debate: a network perspective. *Philos Sci.* 80:356–377.

Corbetta M, Shulman GL. 2002. Control of goal-directed and stimulus-driven attention in the brain. *Nat Rev Neurosci.* 3:201–215.

Crone NE, Korzeniewska A, Franaszczuk PJ. 2011. Cortical gamma responses: searching high and low. *Int J Psychophysiol.* 79:9–15.

Crossley NA, Mechelli A, Vertes PE, Winton-Brown TT, Patel AX, Ginestet CE, McGuire P, Bullmore ET. 2013. Cognitive relevance of the community structure of the human brain functional coactivation network. *Proc Natl Acad Sci U S A.* 110:11583–11588.

Daitch AL, Sharma M, Roland JL, Astafiev SV, Bundy DT, Gaona CM, Snyder AZ, Shulman GL, Leuthardt EC, Corbetta M. 2013. Frequency-specific mechanism links human brain networks for spatial attention. *Proc Natl Acad Sci U S A.* 110:19585–19590.

Dehaene S, Cohen L, Morais J, Kolinsky R. 2015. Illiterate to literate: behavioural and cerebral changes induced by reading acquisition. *Nat Rev Neurosci.* 16:234–244.

Desmurget M, Sirigu A. 2009. A parietal-premotor network for movement intention and motor awareness. *Trends Cogn Sci.* 13:411–419.

Diedrichsen J, Kornysheva K. 2015. Motor skill learning between selection and execution. *Trends Cogn Sci.* 19:227–233.

Duncan J. 2010. The multiple-demand (MD) system of the primate brain: mental programs for intelligent behaviour. *Trends Cogn Sci.* 14:172–179.

Eickhoff SB, Amunts K, Mohlberg H, Zilles K. 2006. The human parietal operculum. II. Stereotaxic maps and correlation with functional imaging results. *Cereb Cortex.* 16:268–279.

Ellis AW. 1988. Normal writing processes and peripheral acquired dysgraphias. *Lang Cogn Process.* 3:99–127.

Engel AK, Gerloff C, Hilgetag CC, Nolte G. 2013. Intrinsic coupling modes: multiscale interactions in ongoing brain activity. *Neuron.* 80:867–886.

Erickson LC, Heeg E, Rauschecker JP, Turkeltaub PE. 2014. An ALE meta-analysis on the audiovisual integration of speech signals. *Hum Brain Mapp.* 35:5587–5605.

Fedorenko E, Thompson-Schill SL. 2014. Reworking the language network. *Trends Cogn Sci.* 18:120–126.

Flinker A, Korzeniewska A, Shestyuk AY, Franaszczuk PJ, Dronkers NF, Knight RT, Crone NE. 2015. Redefining the role of Broca's area in speech. *Proc Natl Acad Sci U S A.* 112:2871–2875.

Fox MD, Snyder AZ, Vincent JL, Corbetta M, Van Essen DC, Raichle ME. 2005. The human brain is intrinsically organized into dynamic, anticorrelated functional networks. *Proc Natl Acad Sci U S A.* 102:9673–9678.

Fries P. 2005. A mechanism for cognitive dynamics: neuronal communication through neuronal coherence. *Trends Cogn Sci.* 9:474–480.

Fuster JM. 2004. Upper processing stages of the perception-action cycle. *Trends Cogn Sci.* 8:143–145.

Graziano MSA. 2016. Ethological action maps: a paradigm shift for the motor cortex. *Trends Cogn Sci.* 20:121–132.

Gross J, Kujala J, Hämäläinen M, Timmermann L, Schnitzler A, Salmelin R. 2001. Dynamic imaging of coherent sources: studying neural interactions in the human brain. *Proc Natl Acad Sci U S A.* 98:694–699.

Gross J, Pollok B, Dirks M, Timmermann L, Butz M, Schnitzler A. 2005. Task-dependent oscillations during unimanual and bimanual movements in the human primary motor cortex and SMA studied with magnetoencephalography. *NeuroImage.* 26:91–98.

Gross J, Timmermann L, Kujala J, Dirks M, Schmitz F, Salmelin R, Schnitzler A. 2002. The neural basis of intermittent motor control in humans. *Proc Natl Acad Sci U S A.* 99: 2299–2302.

Gross J, Timmermann L, Kujala J, Salmelin R, Schnitzler A. 2003. Properties of MEG tomographic maps obtained with spatial filtering. *NeuroImage.* 19:1329–1336.

Haaland KY, Harrington DL, Knight RT. 2000. Neural representations of skilled movement. *Brain.* 123:2306–2313.

Haggard P. 2008. Human volition: towards a neuroscience of will. *Nat Rev Neurosci.* 9:934–946.

Hall TM, de Carvalho F, Jackson A. 2014. A common structure underlies low-frequency cortical dynamics in movement, sleep, and sedation. *Neuron.* 83:1185–1199.

Hannagan T, Amedi A, Cohen L, Dehaene-Lambertz G, Dehaene S. 2015. Origins of the specialization for letters and numbers in ventral occipitotemporal cortex. *Trends Cogn Sci.* 19:374–382.

Hardwick RM, Rottschy C, Miall RC, Eickhoff SB. 2013. A quantitative meta-analysis and review of motor learning in the human brain. *NeuroImage.* 67:283–297.

Hari R, Forss N. 1999. Magnetoencephalography in the study of human somatosensory cortical processing. *Philos Trans R Soc Lond Ser B Biol Sci.* 354:1145–1154.

Harrington DL, Rao SM, Haaland KY, Bobholz JA, Mayer AR, Binderx JR, Cox RW. 2000. Specialized neural systems underlying representations of sequential movements. *J Cogn Neurosci.* 12:56–77.

Hayes JR, Chenoweth NA. 2006. Is working memory involved in the transcribing and editing of texts? *Writ Commun.* 23:135–149.

Hickok G. 2012. Computational neuroanatomy of speech production. *Nat Rev Neurosci.* 13:135–145.

Hogan N, Sternad D. 2007. On rhythmic and discrete movements: reflections, definitions and implications for motor control. *Exp Brain Res.* 181:13–30.

Hommel B, Musseler J, Aschersleben G, Prinz W. 2001. The theory of event coding (TEC): a framework for perception and action planning. *Behav Brain Sci.* 24:849–878.

Ishibashi R, Pobric G, Saito S, Lambon Ralph MA. 2016. The neural network for tool-related cognition: an activation likelihood estimation meta-analysis of 70 neuroimaging contrasts. *Cogn Neuropsychol.* 33:241–256.

Jensen O, Bonnefond M, Marshall TR, Tiesinga P. 2015. Oscillatory mechanisms of feedforward and feedback visual processing. *Trends Neurosci.* 38:192–194.

Jobard G, Crivello F, Tzourio-Mazoyer N. 2003. Evaluation of the dual route theory of reading: a metanalysis of 35 neuroimaging studies. *NeuroImage.* 20:693–712.

Kadmon Harpaz N, Flash T, Dinstein I. 2014. Scale-invariant movement encoding in the human motor system. *Neuron.* 81:452–462.

Katanoda K, Yoshikawa K, Sugishita M. 2001. A functional MRI study on the neural substrates for writing. *Hum Brain Mapp.* 13:34–42.

Kujala J, Gross J, Salmelin R. 2008. Localization of correlated network activity at the cortical level with MEG. *NeuroImage.* 39:1706–1720.

Kujala J, Pammer K, Cornelissen P, Roebroeck A, Formisano E, Salmelin R. 2007. Phase coupling in a cerebro-cerebellar network at 8-13 Hz during reading. *Cereb Cortex.* 17:1476–1485.

Lacadie CM, Fulbright RK, Rajeevan N, Constable RT, Papademetris X. 2008. More accurate talairach coordinates for neuroimaging using non-linear registration. *NeuroImage.* 42:717–725.

Lashley KS. 1951. The problem of serial order in behavior. In: Jeffres LA, editor. *Cerebral mechanisms in behavior.* New York (NY): Wiley, pp. 112–146.

Liebe S, Hoerzer GM, Logothetis NK, Rainer G. 2012. Theta coupling between V4 and prefrontal cortex predicts visual short-term memory performance. *Nat Neurosci.* 15:456–462.

Liljeström M, Kujala J, Jensen O, Salmelin R. 2005. Neuromagnetic localization of rhythmic activity in the human brain: a comparison of three methods. *NeuroImage.* 25:734–745.

Liljeström M, Kujala J, Stevenson C, Salmelin R. 2015. Dynamic reconfiguration of the language network preceding onset of speech in picture naming. *Hum Brain Mapp.* 36:1202–1216.

Liljeström M, Vartiainen J, Kujala J, Salmelin R. 2018. Large-scale functional networks connect differently for processing words and symbol strings. *PLoS One.* 13:e0196773.

Linderman M, Lebedev MA, Erlichman JS. 2009. Recognition of handwriting from electromyography. *PLoS One.* 4:e6791.

Manganotti P, Gerloff C, Toro C, Katsuta H, Sadato N, Zhuang P, Leocani L, Hallett M. 1998. Task-related coherence and task-related spectral power changes during sequential finger movements. *Electroencephalogr Clin Neurophysiol.* 109: 50–62.

Maris E, Fries P, van Ede F. 2016. Diverse phase relations among neuronal rhythms and their potential function. *Trends Neurosci.* 39:86–99.

Martínez-Vázquez P, Gail A. 2018. Directed interaction between monkey premotor and posterior parietal cortex during motor-goal retrieval from working memory. *Cereb Cortex.* 28:1866–1881.

Mayka MA, Corcos DM, Leurgans SE, Vaillancourt DE. 2006. Three-dimensional locations and boundaries of motor and premotor cortices as defined by functional brain imaging: a meta-analysis. *NeuroImage.* 31:1453–1474.

Meunier D, Lambiotte R, Fornito A, Ersche KD, Bullmore ET. 2009. Hierarchical modularity in human brain functional networks. *Front Neuroinform.* 3:37.

Miller KJ, Hermes D, Honey CJ, Hebb AO, Ramsey NF, Knight RT, Ojemann JG, Fetz EE. 2012. Human motor cortical activity is selectively phase-entrained on underlying rhythms. *PLoS Comput Biol.* 8:e1002655.

Nichols TE, Holmes AP. 2002. Nonparametric permutation tests for functional neuroimaging: a primer with examples. *Hum Brain Mapp.* 15:1–25.

Omura K, Tsukamoto T, Kotani Y, Ohgami Y, Yoshikawa K. 2004. Neural correlates of phoneme-to-grapheme conversion. *Neuroreport.* 15:949–953.

Oswal A, Beudel M, Zrinzo L, Limousin P, Hariz M, Foltynie T, Litvak V, Brown P. 2016. Deep brain stimulation modulates synchrony within spatially and spectrally distinct resting state networks in Parkinson's disease. *Brain.* 139:1482–1496.

Pacherie E. 2008. The phenomenology of action: a conceptual framework. *Cognition*. 107:179–217.

Palva JM, Monto S, Kulashekhar S, Palva S. 2010. Neuronal synchrony reveals working memory networks and predicts individual memory capacity. *Proc Natl Acad Sci U S A*. 107:7580–7585.

Pesaran B, Nelson MJ, Andersen RA. 2008. Free choice activates a decision circuit between frontal and parietal cortex. *Nature*. 453:406–409.

Petersen SE, Sporns O. 2015. Brain networks and cognitive architectures. *Neuron*. 88:207–219.

Planton S, Jucla M, Roux FE, Demonet JF. 2013. The "handwriting brain": a meta-analysis of neuroimaging studies of motor versus orthographic processes. *Cortex*. 49:2772–2787.

Planton S, Longcamp M, Péran P, Démonet JF, Jucla M. 2017. How specialized are writing-specific brain regions? An fMRI study of writing, drawing and oral spelling. *Cortex*. 88:66–80.

Polania R, Nitsche MA, Korman C, Batsikadze G, Paulus W. 2012. The importance of timing in segregated theta phase-coupling for cognitive performance. *Curr Biol*. 22:1314–1318.

Pollok B, Gross J, Muller K, Aschersleben G, Schnitzler A. 2005. The cerebral oscillatory network associated with auditorily paced finger movements. *NeuroImage*. 24:646–655.

Potgieser AR, van der Hoorn A, de Jong BM. 2015. Cerebral activations related to writing and drawing with each hand. *PLoS One*. 10:e0126723.

Purcell JJ, Turkeltaub PE, Eden GF, Rapp B. 2011. Examining the central and peripheral processes of written word production through meta-analysis. *Front Psychol*. 2:239.

Raichle ME. 2015. The brain's default mode network. *Annu Rev Neurosci*. 38:433–447.

Raij T, Uutela K, Hari R. 2000. Audiovisual integration of letters in the human brain. *Neuron*. 28:617–625.

Ramayya AG, Glasser MF, Rilling JK. 2010. A DTI investigation of neural substrates supporting tool use. *Cereb Cortex*. 20:507–516.

Rhodes BJ, Bullock D, Verwey WB, Averbeck BB, Page MP. 2004. Learning and production of movement sequences: behavioral, neurophysiological, and modeling perspectives. *Hum Mov Sci*. 23:699–746.

Rijntjes M, Dettmers C, Buchel C, Kiebel S, Frackowiak RS, Weiller C. 1999. A blueprint for movement: functional and anatomical representations in the human motor system. *J Neurosci*. 19:8043–8048.

Rizzolatti G, Sinigaglia C. 2016. The mirror mechanism: a basic principle of brain function. *Nat Rev Neurosci*. 17:757–765.

Roby-Brami A, Hermsdörfer J, Roy AC, Jacobs S. 2012. A neuropsychological perspective on the link between language and praxis in modern humans. *Philos Trans R Soc Lond Ser B Biol Sci*. 367:144–160.

Roelfsema PR, Engel AK, Konig P, Singer W. 1997. Visuomotor integration is associated with zero time-lag synchronization among cortical areas. *Nature*. 385:157–161.

Rohenkohl G, Bosman CA, Fries P. 2018. Gamma synchronization between V1 and V4 improves behavioral performance. *Neuron*. 100:953–963.

Rottschy C, Langner R, Dogan I, Reetz K, Laird AR, Schulz JB, Fox PT, Eickhoff SB. 2012. Modelling neural correlates of working memory: a coordinate-based meta-analysis. *NeuroImage*. 60:830–846.

Roux FE, Dufor O, Giussani C, Wamain Y, Draper L, Longcamp M, Demonet JF. 2009. The graphemic/motor frontal area Exner's area revisited. *Ann Neurol*. 66:537–545.

Roux FE, Durand JB, Rehault E, Planton S, Draper L, Demonet JF. 2014. The neural basis for writing from dictation in the temporoparietal cortex. *Cortex*. 50:64–75.

Ruspantini I, Saarinen T, Belardinelli P, Jalava A, Parviainen T, Kujala J, Salmelin R. 2012. Corticomuscular coherence is tuned to the spontaneous rhythmicity of speech at 2-3 Hz. *J Neurosci*. 32:3786–3790.

Saarinen T, Jalava A, Kujala J, Stevenson C, Salmelin R. 2015. Task-sensitive reconfiguration of corticocortical 6-20 Hz oscillatory coherence in naturalistic human performance. *Hum Brain Mapp*. 36:2455–2469.

Salazar RF, Dotson NM, Bressler SL, Gray CM. 2012. Content-specific fronto-parietal synchronization during visual working memory. *Science*. 338:1097–1100.

Salmelin R, Hämäläinen M, Kajola M, Hari R. 1995. Functional segregation of movement-related rhythmic activity in the human brain. *NeuroImage*. 2:237–243.

Sarnthein J, Petsche H, Rappelsberger P, Shaw GL, von Stein A. 1998. Synchronization between prefrontal and posterior association cortex during human working memory. *Proc Natl Acad Sci U S A*. 95:7092–7096.

Scaltritti M, Pinet S, Longcamp M, Alario FX. 2017. On the functional relationship between language and motor processing in typewriting: an EEG study. *Lang Cogn Neurosci*. 32:1086–1101.

Schoffelen JM, Gross J. 2009. Source connectivity analysis with MEG and EEG. *Hum Brain Mapp*. 30:1857–1865.

Schönle PW, Hong G, Benecke R, Conrad B. 1986. Aspects of speech motor control: programing of repetitive versus non-repetitive speech. *Neurosci Lett*. 63:170–174.

Schormann T, Henn S, Zilles K. 1996. A new approach to fast elastic alignment with applications to human brains. In: Höhne KH, Kikinis R, editors. *Visualization in biomedical computing. VBC 1996. Lecture notes in computer science*. Vol Vol. 1131. Berlin: Springer, pp. 337–342.

Segal E, Petrides M. 2012. The anterior superior parietal lobule and its interactions with language and motor areas during writing. *Eur J Neurosci*. 35:309–322.

Sepulcre J, Sabuncu MR, Yeo TB, Liu H, Johnson KA. 2012. Stepwise connectivity of the modal cortex reveals the multimodal organization of the human brain. *J Neurosci*. 32:10649–10661.

Shima K, Isoda M, Mushiake H, Tanji J. 2007. Categorization of behavioural sequences in the prefrontal cortex. *Nature*. 445:315–318.

Siegel M, Donner TH, Engel AK. 2012. Spectral fingerprints of large-scale neuronal interactions. *Nat Rev Neurosci*. 13:121–134.

Singer W. 2013. Cortical dynamics revisited. *Trends Cogn Sci*. 17:616–626.

Sugihara G, Kaminaga T, Sugishita M. 2006. Interindividual uniformity and variety of the "writing center": a functional MRI study. *NeuroImage*. 32:1837–1849.

Szczepanski SM, Crone NE, Kuperman RA, Auguste KI, Parvizi J, Knight RT. 2014. Dynamic changes in phase-amplitude coupling facilitate spatial attention control in fronto-parietal cortex. *PLoS Biol*. 12:e1001936.

Tanji J. 2001. Sequential organization of multiple movements: involvement of cortical motor areas. *Annu Rev Neurosci*. 24:631–651.

Tarkiainen A, Helenius P, Hansen PC, Cornelissen PL, Salmelin R. 1999. Dynamics of letter string perception in the human occipitotemporal cortex. *Brain*. 122:2119–2132.

Tass P, Rosenblum MG, Weule J, Kurths J, Pikovsky A, Volkmann J, Schnitzler A, Freund HJ. 1998. Detection of n:m phase locking from noisy data: application to magnetoencephalography. *Phys Rev Lett*. 81:3291–3294.

Taulu S, Simola J. 2006. Spatiotemporal signal space separation method for rejecting nearby interference in MEG measurements. *Phys Med Biol*. 51:1759–1768.

Thomassen AJ, Meulenbroek RG. 1998. Low-frequency periodicity in the coordination of progressive handwriting. *Acta Psychol (Amst)*. 100:133–144.

Thorne JD, De Vos M, Viola FC, Debener S. 2011. Cross-modal phase reset predicts auditory task performance in humans. *J Neurosci*. 31:3853–3861.

Turesky TK, Turkeltaub PE, Eden GF. 2016. An activation likelihood estimation meta-analysis study of simple motor movements in older and young adults. *Front Aging Neurosci*. 8:238.

Turken AU, Dronkers NF. 2011. The neural architecture of the language comprehension network: converging evidence from lesion and connectivity analyses. *Front Syst Neurosci*. 5:1.

van Atteveldt N, Formisano E, Goebel R, Blomert L. 2004. Integration of letters and speech sounds in the human brain. *Neuron*. 43:271–282.

van Polanen V, Davare M. 2015. Interactions between dorsal and ventral streams for controlling skilled grasp. *Neuropsychologia*. 79:186–191.

van Vliet M, Liljeström M, Aro S, Salmelin R, Kujala J. 2018. Analysis of functional connectivity and oscillatory power using DICS: from raw MEG data to group-level statistics in python. *Front Neurosci*. 12:586.

Varela F, Lachaux JP, Rodriguez E, Martinerie J. 2001. The brainweb: phase synchronization and large-scale integration. *Nat Rev Neurosci*. 2:229–239.

Verwey WB, Shea CH, Wright DL. 2015. A cognitive framework for explaining serial processing and sequence execution strategies. *Psychon Bull Rev*. 22:54–77.

Vigneau M, Beaucousin V, Herve PY, Duffau H, Crivello F, Houde O, Mazoyer B, Tzourio-Mazoyer N. 2006. Meta-analyzing left hemisphere language areas: phonology, semantics, and sentence processing. *NeuroImage*. 30:1414–1432.

von Stein A, Sarnthein J. 2000. Different frequencies for different scales of cortical integration: from local gamma to long range alpha/theta synchronization. *Int J Psychophysiol*. 38:301–313.

Wang XJ. 2010. Neurophysiological and computational principles of cortical rhythms in cognition. *Physiol Rev*. 90:1195–1268.

Watrous AJ, Tandon N, Conner CR, Pieters T, Ekstrom AD. 2013. Frequency-specific network connectivity increases underlie accurate spatiotemporal memory retrieval. *Nat Neurosci*. 16:349–356.

Witt ST, Laird AR, Meyerand ME. 2008. Functional neuroimaging correlates of finger-tapping task variations: an ALE meta-analysis. *NeuroImage*. 42:343–356.

Wolpert DM, Ghahramani Z. 2000. Computational principles of movement neuroscience. *Nat Neurosci*. 3:1212–1217.

Womelsdorf T, Valiante TA, Sahin NT, Miller KJ, Tiesinga P. 2014. Dynamic circuit motifs underlying rhythmic gain control, gating and integration. *Nat Neurosci*. 17:1031–1039.

Wymbs NF, Bassett DS, Mucha PJ, Porter MA, Grafton ST. 2012. Differential recruitment of the sensorimotor putamen and frontoparietal cortex during motor chunking in humans. *Neuron*. 74:936–946.

Xu Y, Lin Q, Han Z, He Y, Bi Y. 2016. Intrinsic functional network architecture of human semantic processing: modules and hubs. *NeuroImage*. 132:542–555.

Yuan Y, Brown S. 2015. Drawing and writing: an ALE meta-analysis of sensorimotor activations. *Brain Cogn*. 98:15–26.